Experimental and theoretical studies of the displacement of a hydrodynamic supported idle spindle of a three-spindle screw pump

Dipl.-Ing. Joachim Thurner
Institut für Fluidsystemtechnik (FST), Technische Universität Darmstadt, Magdalenenstraße 4, 64289 Darmstadt, Email: joachim.thurner@fst.tu-darmstadt.de

Professor Dr.-Ing. Peter Pelz
Institut für Fluidsystemtechnik (FST), Technische Universität Darmstadt, Magdalenenstraße 4, 64289 Darmstadt, Email: peter.pelz@fst.tu-darmstadt.de

Dipl.-Ing. Frank Holz
Leistritz Pumpen GmbH, Marktgrafenstraße 29-39, 90459 Nürnberg, Email: fholz@leistritz.com

Abstract

The bending and displacement of a hydrodynamic supported idle screw of a 3-spindle screw pump is measured by a set of inductive sensors. The experimental results are compared with a coupled fluid and structure model. The idle screw is modeled as a Bernoulli beam interacting with a hydrodynamic lubrication film.

Introduction

Screw pumps are kinematic pulsation free positive displacement pumps. The hydrodynamic supported sidewise idle spindles are driven by engagement of the center drive spindle (**Figure 1**). In unpropitious operation points of low rotating speed, low viscosity and high pressure difference contact between the idle spindle and the casing may occur. State of the art, is to detect this operation limit experimentally. The aim of the present research is to improve the physical understanding of the problem and to give a theoretical approach of this operation limit.

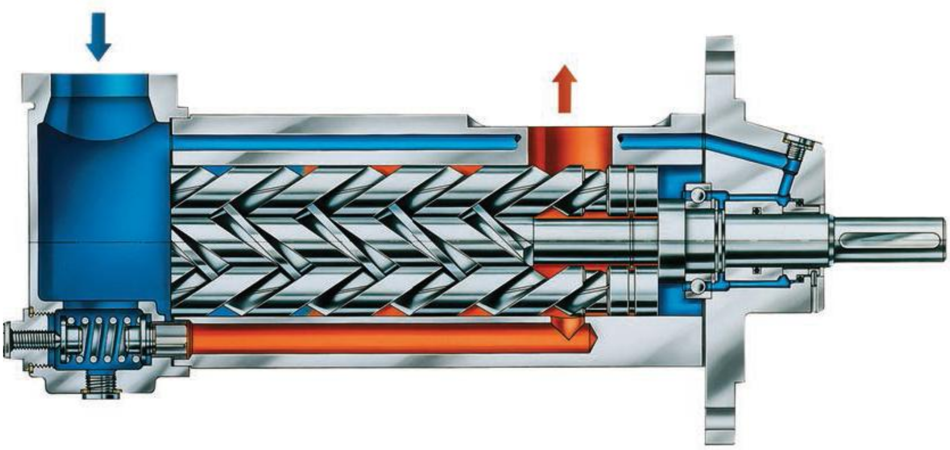

Figure 1: 3-spindle screw pump, Leistritz Pumpen GmbH

Experimental setup

Former experimental studies leaded to the conclusion that the movement of the idle screw can't be understood as a rigid body movement. Bending aspects have to be taken into account [3]. Therefore a set of four inductive distance sensors was placed along the idle spindle axis. The axial distance of the sensors is equal to the pitch of the idle screw. The sensor head is embedded in a magnetic inert sealing elastomer plug, which is shaped to the casing contour. The sensor and the plug are hold in position by a brass screw (**Figure 2**).

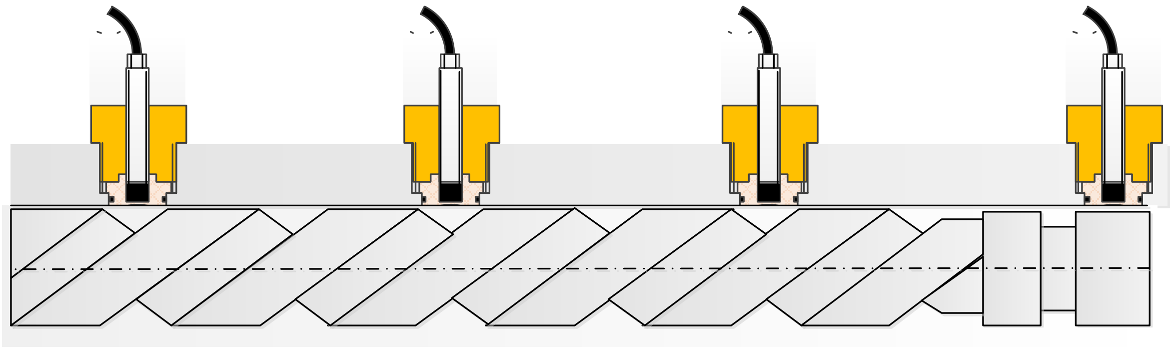

Figure 2: Axial sensor positions

For horizontal and vertical displacement measurement the system is applied in two perpendicular measurement planes. (**Figure 3**).

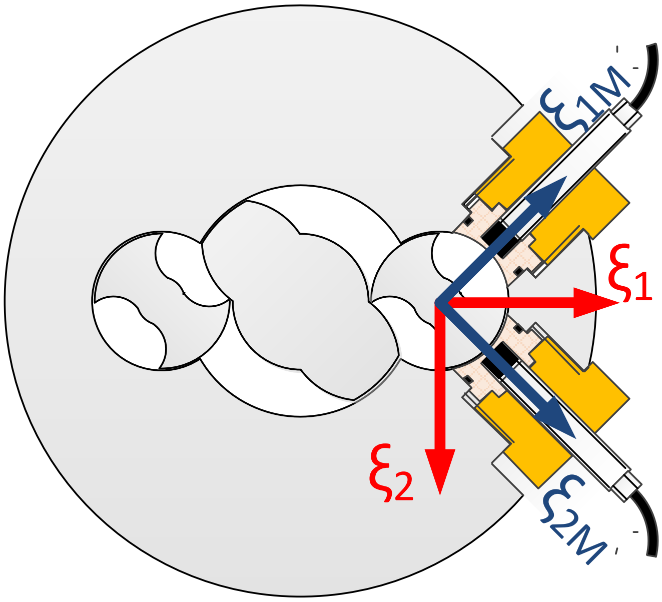

Figure 3: Coordinate systems, view from suction side

Due to the fact that an absolute changeless calibration of the center of the screw to the center of the housing is impossible, the origin of coordinates is defined by an initial point of operation, which has to be reproduced every measurement series. Experience shows that the measurement results are reproducible.

Hydrodynamic model

The pressure and shear load, p and τ, on the idle screw is modeled by 2-dimensional lubrication theory, given by Reynolds equation

$$\nabla\cdot\ \ \frac{h^3}{\mu}\nabla p\ \ = 6\nabla\cdot\ \ hU_1 + hU_2\ \ + 12\frac{\partial h}{\partial t} \qquad (1)$$

and shear equation

$$\tau = \frac{\mu}{h}\ \ U_2 - U_1\ \ - \frac{h}{2}\nabla p, \qquad (2)$$

with gap height h, dynamic viscosity μ, spindle wall speed U_1, opposite wall speed U_2, time t, and surface normal n, leading to the 3-dimenional stress vector on the spindle surface

$$t = -pn + \tau. \qquad (3)$$

Figure 4 shows the pressure deviation of a standard operation point with a dynamic viscosity μ of 5 mPas, a rotating speed of 3000 rpm and a pressure difference Δp of 39 bar, on the left side on the 2D-projection of the geometry, on the right side on the spindle surface. Leakage between drive and idle spindle is not taken into account, which is reasonable for having rotor dynamics in focus and not volumetric efficiency of the pump [1] [2] [4].

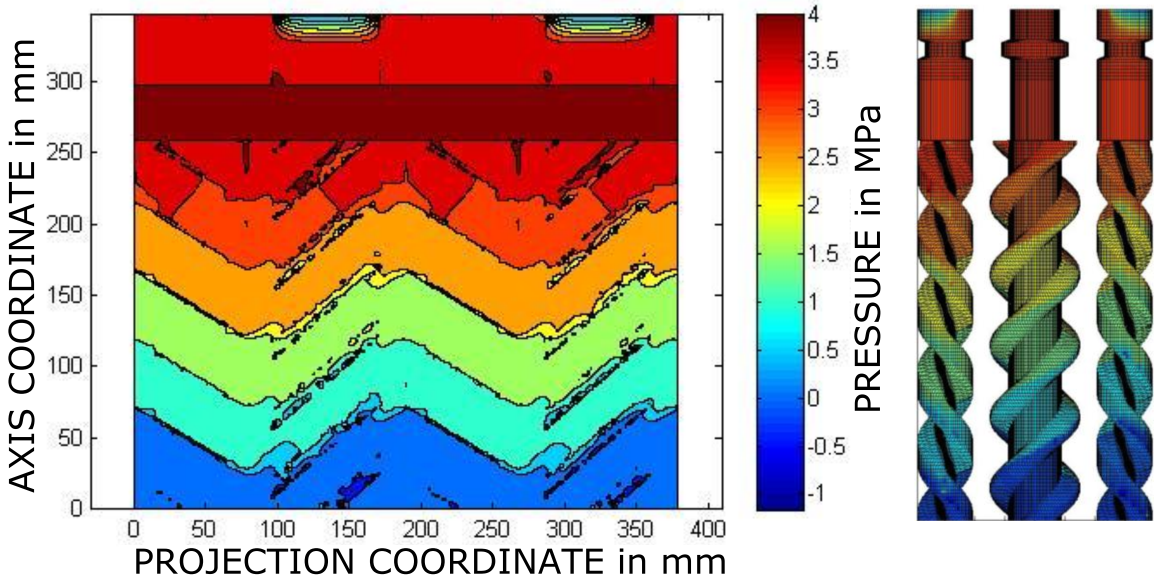

Figure 4: pressure deviation in standard operation point

We take advantage of the linearity of Reynolds and shear equation in pressure p, shear stress τ and various speed terms. The influence of pressure difference, rotating speed and lateral spindle displacement can be handled separately.

The homogenious solution of Reynolds equation can be scaled by pressure difference and suction pressure p_0.

$$p_1 = p_1\ \ \Delta p = 1, \varphi, \xi_1, \xi_2\ \ \Delta p + p_0. \qquad (4)$$

Unfortunately it is a nonlinear function of turn angle φ and displacement ξ_1 and ξ_2, due to the non-linear influence of gap height h. **Figure 5** shows p_1 separately.

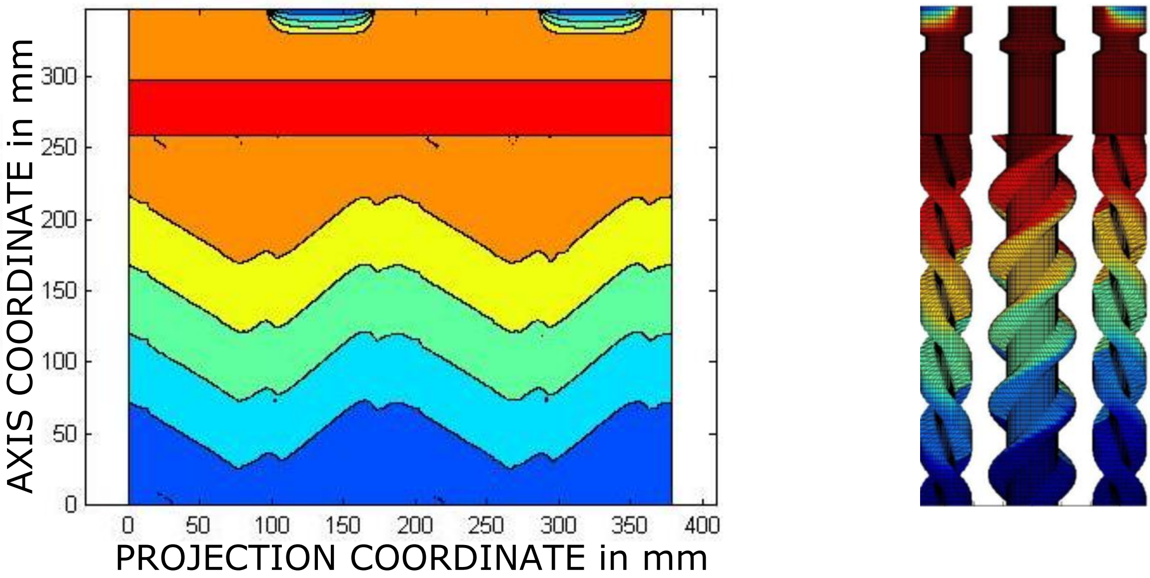

Figure 5: 1st fundamental solution, influence of pressure difference

The most important inhomogeneous solution results from angular speed Ω and viscosity μ.

$$p_2 = p_2 \ \ \mu\Omega = 1, \varphi, \xi_1, \xi_2 \ \ \mu\Omega. \tag{5}$$

In **Figure 6** the idle spindles are deviated in ξ_1-direction. The typical pressure deviation of the journal bearing effect can be seen.

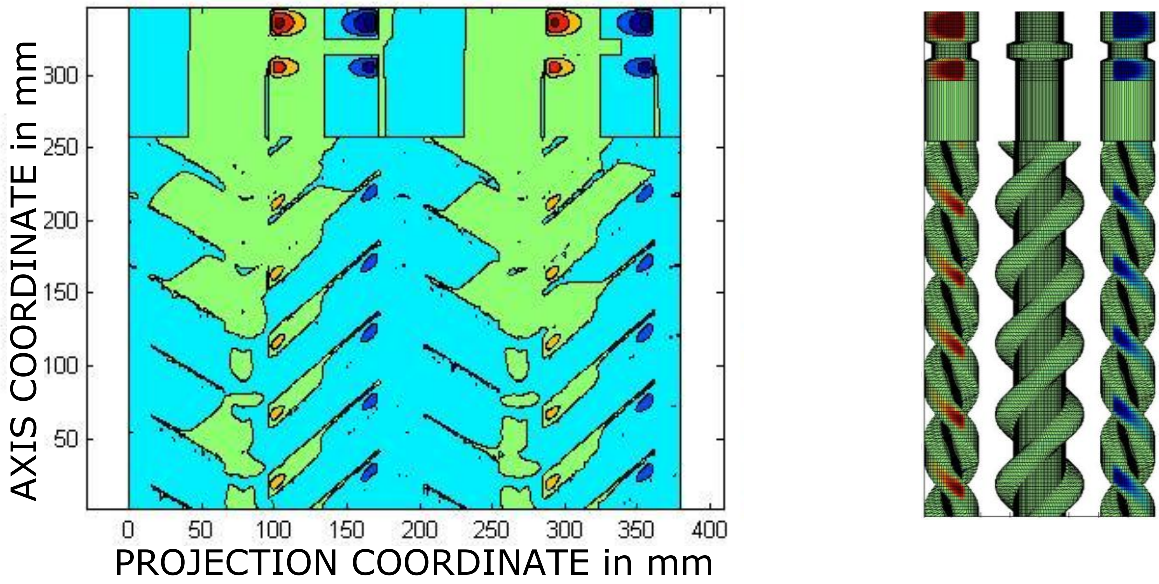

Figure 6: 2nd fundamental solution, influence of rotating speed

Further fundamental solutions are given by displacement speeds ξ_1 and ξ_2. Due to our measurement results, transient aspects are less important for the understanding of the deviation problem, so we disclaim presenting them here.

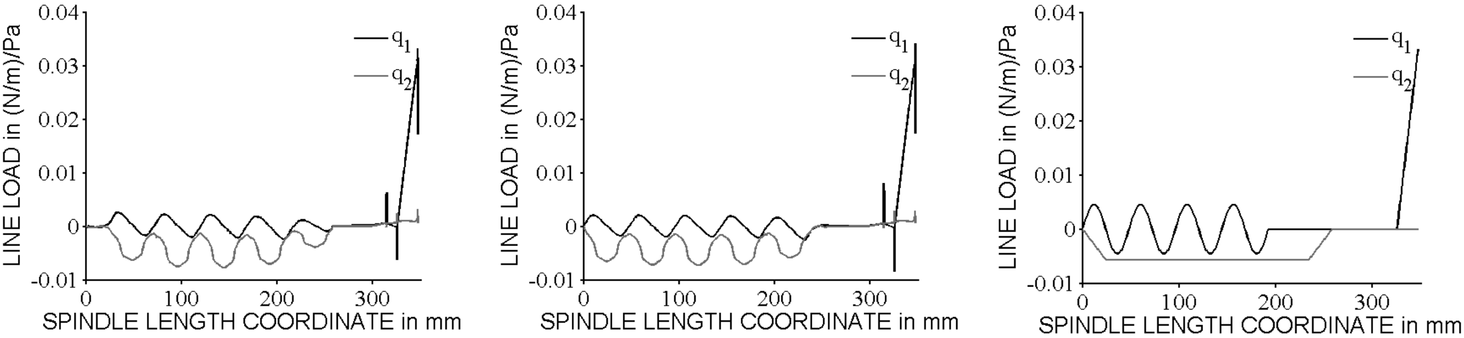

Figure 7: Line load diagrams for $\varphi = 0°$ and $\varphi = 90°$ and simplified for bending line model

Bending line model

From the simulation results line load functions q can be generated. **Figure 7** shows line load diagrams of the idle spindle pressure solution for different turn angles. Although the deviation of the line load is different due to different chamber positions, the resulting radial force in ξ_2-direction from the screw geometry section of the spindle is the same. For that component exists an analytical solution from Hamelberg [5] which is approved by 3D-CFD-simulations. Due to geometric inaccuracy the simulated forces from 2D-lubrication theory are a bit to small. The radial force from screw geometry in ξ_1-direction is zero in sum. The line load peak in ξ_1-direction on the discharge side of the spindle is conditioned from the design of the sealing system (see also Figures 1, 4, 5). The bending line model works with simplified line load functions.

The bending line is given by the Bernoulli beam equation in coordinate direction i

$$EI_i \xi_i{}''{}'' = q_i, \qquad (6)$$

and its boundary conditions at both spindle ends

$$EI_i \xi_{i\,end}{}'' = EI_i \xi_{i\,end}{}''{}' = 0. \qquad (7)$$

The line load is given by pressure difference line load q_{iP} and rotating speed line load q_{iJ} representing the jounal bearing effect, given.

$$q_i = q_{iP} + q_{iJ}(\xi_j, \mu, \Omega). \qquad (8)$$

The problem was solved numerically and iterative.

Results

Due to the fact that a changeless calibration is not possible with the measurement system, the displacement is referred to an operation point of 2 bar, 1500 rpm and an oil temperature of 30°C, that leads to a dynamic viscosity of 5 mPas. For three test series, the result is plotted in **Figure 8**. 8a shows a series that was done with a constant rotating speed of 1500 rpm and various pressures. In the ξ_{1M}-direction the idle spindle moves towards the casing wall with rising pressure. In ξ_{2M}-direction a cardanic displacement in combination with a strong bending influence can be seen. The simulation resuls in Figure 8b reproduces the measurement results qualitatively. Another measurement series was done at 1000 rpm. The behavior is nearly the same. Those measurements were done only till 40 bar with regard to operation limits of the pump within this fluidic hydraulic oil. A third measurement series was done at 30 bar and 1500 rpm. By warming the oil the viscosity declined. Here as well the basic behavior could be reproduced by simulations [6].

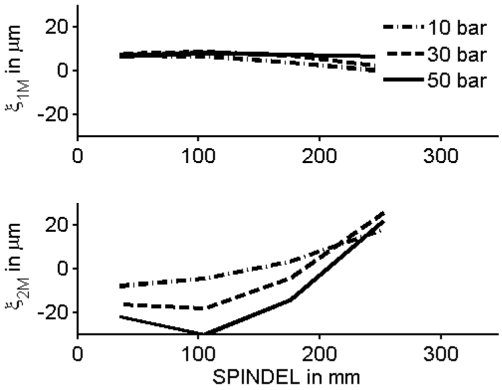

Figure 8a: 1500 rpm, 30°C measured

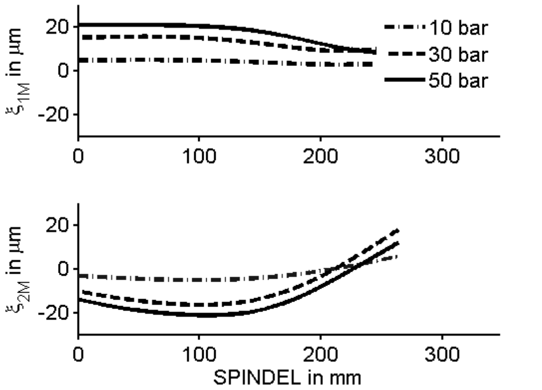

Figure 8b: 1500 rpm, 5 mPas simulated

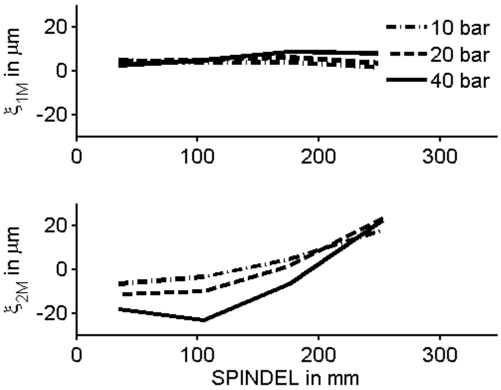

Figure 8c: 1000 rpm, 30°C measured

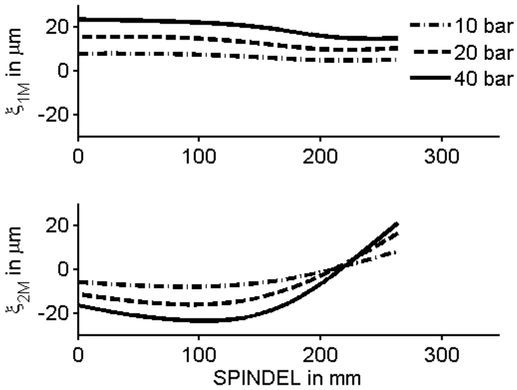

Figure 8d: 1000 rpm, 5 mPas simulated

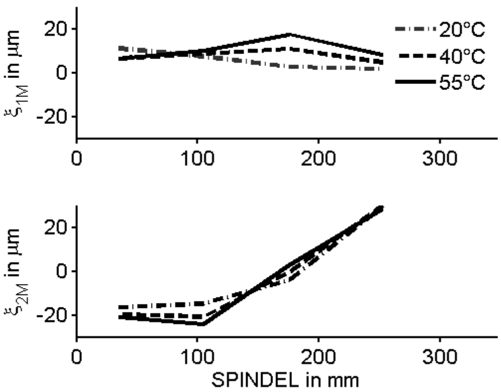

Figure 8e: 1500 rpm, 30 bar measured

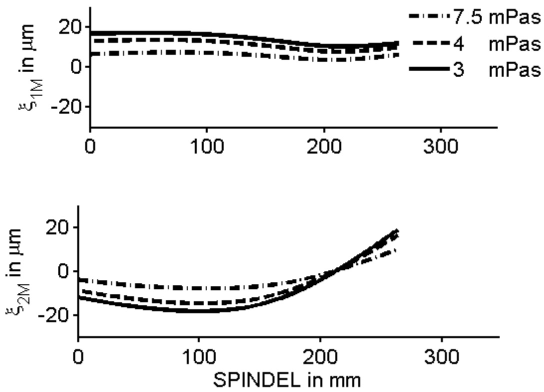

Figure 8f: 1500 rpm, 30 bar simulated

Acknowldgement
We want to thank the employees of Leistritz Pumpen GmbH for their support to our scientific project with their experience, their time and with components.

List of Symbols

p	pressure
Δp	pressure difference
p_0	suction pressure
h	gap height
μ	dynamic viscosity
U_1	spindle wall speed
U_2	opposite wall speed
t	time
τ	2D shear vector
t	stress vector
n	spindle surface normal
φ	turn angle
Ω	angular speed
ξ	displacement
ξ_1	horizontal displacement
ξ_2	vertical displacement
E	elastic modulus
I_i	geometrical moment of inertia
q_i	line load
q_1	horizontal line load
q_2	vertical line load
q_{iP}	pressure indicated line load
q_{iJ}	journal bearing line load

References

[1] Bevern, S., Thurner, J., Pelz, P., Holz, F.: Das dynamische Betriebsverhalten von Schrauben-pumpen – ein neuer innovativer Berechnungsansatz, 8. VDI-Fachtagung Schraubenmaschinen 2010

[2] Bevern, S: Spaltströmungen und daraus resultierende Kräfte bei Spindelpumpen, TU Darmstadt, Bachelorarbeit 2009

[3] Rossow, P: Experimentelle Untersuchung der Verlagerung gleitgelagerter Schraubenpumpen-Rotoren, TU Darmstadt, Bachelorarbeit 2011

[4] Spurk, J., Aksel, N.: Strömungslehre, Einführung in die Theorie der Strömungen, 7 Auflage, Springer-Verlag Berlin Heidelberg 2007

[5] Hamelberg, F: Läuferkräfte bei Schraubenpumpen, Dissertation Technische Hochschule Hannover, 1966

[6] Stockert, S: Experimentelle Untersuchung der Biegelinie gleitgelagerter Schraubenpumpen-Rotoren, Bachelorarbeit 2012